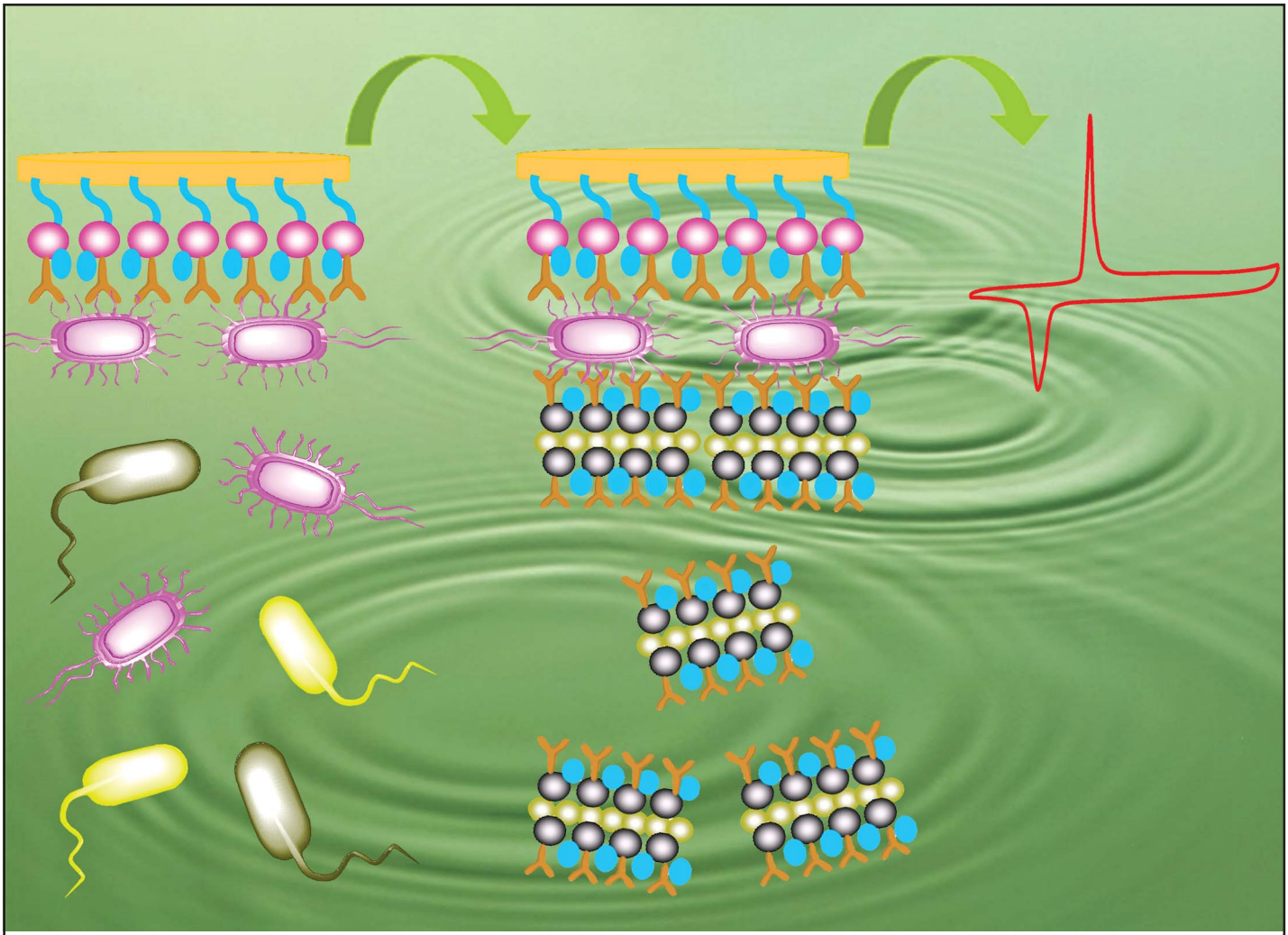

Showcasing electrochemical immunoassay for *Escherichia coli* from the Nano-Bioanalytic Laboratory of Professor Heyou Han at the College of Science, State Key Laboratory of Agricultural Microbiology, Huazhong Agricultural University, Wuhan, P.R. China.

Title: Solid-state voltammetry based electrochemical immunosensor for *Escherichia coli* using graphene oxide–Ag nanoparticle composites as labels

A new electrochemical immunosensor for *Escherichia coli* (*E. coli*) was fabricated based on solid-state voltammetry by using graphene oxide–Ag nanoparticle nanocomposites (P-GO–Ag) as labels, and the biosensor was applied to monitor *E. coli* in lake water with satisfactory results.

As featured in:

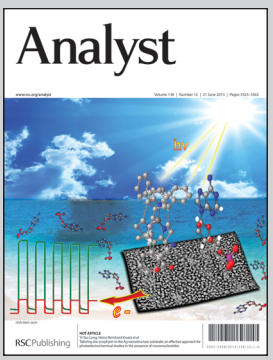

See Heyou Han *et al.*, *Analyst*, 2013, **138**, 3388–3393.

RSC Publishing

www.rsc.org/analyst

Registered Charity Number 207890

Analyst

RSC Publishing

PAPER

View Article Online
View Journal | View Issue

Solid-state voltammetry-based electrochemical immunosensor for *Escherichia coli* using graphene oxide–Ag nanoparticle composites as labels†

Cite this: *Analyst*, 2013, **138**, 3388

Xiaochun Jiang, Kun Chen, Jing Wang, Kang Shao, Tao Fu, Feng Shao, Donglian Lu, Jiangong Liang, M. Frahat Foda and Heyou Han*

A new electrochemical immunosensor based on solid-state voltammetry was fabricated for the detection of *Escherichia coli* (*E. coli*) by using graphene oxide–Ag nanoparticle composites (P-GO–Ag) as labels. To construct the platform, Au nanoparticles (AuNPs) were first self-assembled on an Au electrode surface through cysteamine and served as an effective matrix for antibody (Ab) attachment. Under a sandwich-type immunoassay format, the analyte and the probe (P-GO–Ag–Ab) were successively captured onto the immunosensor. Finally, the bonded AgNPs were detected through a solid-state redox process in 0.2 M of KCl solution. Combining the advantages of the high-loading capability of graphene oxide with promoted electron-transfer rate of AuNPs, this immunosensor produced a 26.92-fold signal enhancement compared with the unamplified protocol. Under the optimal conditions, the immunosensor exhibited a wide linear dependence on the logarithm of the concentration of *E. coli* ranging from 50 to 1.0×10^6 cfu mL^{-1} with a detection limit of 10 cfu mL^{-1}. Moreover, as a practical application, the proposed immunosensor was used to monitor *E. coli* in lake water with satisfactory results.

Received 8th January 2013
Accepted 11th April 2013

DOI: 10.1039/c3an00056g

www.rsc.org/analyst

Introduction

Escherichia coli (*E. coli*), which is found in large numbers in the intestine of humans and other warm-blooded animals, is widely distributed in natural environment. Most of the strains are harmless, but some serotypes can cause bacterial infections including cholecystitis, bacteremia, cholangitis, urinary tract infection and other clinical infections such as neonatal meningitis and pneumonia.[1] *E. coli* is a common type of microorganism for microbial contamination in water, and can reliably reflect fecal contamination.[1,2] So it has been extensively used as an indicator organism for water quality and its routine monitoring is used to protect people from bacterial infections in many countries.

Several conventional microbiological methods such as plate counting,[3] multiple-tube fermentation,[4] the membrane filter technique[5] and turbidimetry[6] have been used for the determination of *E. coli*. These methods are of high accuracy, but usually need a relatively long detection period (more than 24 h) and complex operating procedures. More importantly, some of them are less sensitive and specific. Therefore, much effort should be devoted to the development of some simple, selective and sensitive detection techniques for *E. coli* in environmental monitoring, the food industry and cliniccal chemistry. Currently, some new strategies including the quartz crystal microbalance,[7] surface plasmon resonance,[8] photochemistry[9] and electrochemistry[10–12] have been proposed as alternatives to conventional methods for detecting *E. coli*.

Among them, the electrochemical immunoassay has attracted considerable interest because of its unique properties such as simplicity, speediness, accuracy, low cost and portability.[13] In order to increasing the sensitivity of detection for *E. coli*, three kinds of signal amplification technologies using nanomaterials[14] have been proposed: (1) metal nanoparticles such as Au nanoparticles (AuNPs) are adopted to increase the electron-transfer rate and the effective area of the working electrode to amplify the signal;[15] (2) metal nanoparticles (Cu@Au nanoparticles) are directly used as electroactive labels to amplify the electrochemical responses;[12] and (3) nanoparticles are used as carriers to load a large amount of electroactive species for signal amplification.[11] This aroused our interest in seeking other nanomaterials as signal amplifiers for the sensitive detection of *E. coli*. Recently, graphene oxide (GO) was well recognized as a popularly used nanocarrier to load a large number of labels due to its large surface area, high loading ratio, good biocompatibility and physiological stability.[16–19] Du *et al.* employed GO as a nanocarrier to successfully propose a multienzyme amplification strategy for the ultrasensitive electrochemical immunoassay of phosphorylated p53 (S392).[18] Zhu and co-workers

State Key Laboratory of Agricultural Microbiology, College of Science, Huazhong Agricultural University, Wuhan 430070, P.R. China. E-mail: hyhan@mail.hzau.edu.cn; Fax: +86-27-87288246; Tel: +86-27-87288246

† Electronic supplementary information (ESI) available. See DOI: 10.1039/c3an00056g

adopted a GO-based nanoprobe to realize the sensitive detection of human IgG.[17] However, as far as we know, the electrochemical immunoassay of *E. coli* using GO as a nanocarrier for signal amplification has not been reported.

Solid-state voltammetry is the use of the voltammetric technique to investigate the electrochemistry of surface-confined electroactive micro/nanocrystals in contact with an electrolyte medium. The solid-state Ag/AgCl process is a typical form of solid-state voltammetry. Compared with stripping voltammetry, it can bring on a larger peak current at a lower potential (about +0.1 V *vs.* Ag/AgCl electrode), which is far from unwanted oxidative interferences.[20–22] These unique advantages have intrigued many researchers to develop biosensors based on solid-state voltammetry. Ying's group first used solid-state voltammetry to detect prostate-specific antigen[21] and the DNA oligonucleotide of the avian flu virus H5N1.[20,22] Then, Ju and his colleagues adopted this voltammetry for the ultrasensitive determination of tumor markers.[23] Most recently, our group also developed a sensitive biosensor for *Bacillus thuringiensis* transgenic sequence detection by using solid-state voltammetry.[24]

Herein, we present a direct electrochemical immunosensor for *E. coli* assay using graphene oxide–Ag nanoparticle composites (P-GO–Ag) as labels. In this case, solid-state voltammetry was adopted for the detection of *E. coli* for the first time. The detection scheme is shown in Fig. 1. AuNPs were first immobilized on an Au electrode. The introduction of AuNPs not only provided an effective matrix for antibody (Ab) immobilization but also increased the electron-transfer rate. The nanoprobe (P-GO–Ag–Ab) was designed by assembling Ab on P-GO–Ag and then captured on the electrode surface *via* a sandwich-type immunoreaction. With solid-state voltammetry, the constructed immunosensor showed a good analytical performance for *E. coli* in both buffer solution and lake water.

Experimental

Chemicals and materials

Anti-*E. coli* polyclonal antibody (Ab) was obtained from Abcam (Cambridge, UK). Bovine serum albumin (BSA) and poly(diallyldimethylammonium chloride) (PDDA) (M_w = 40 000–50 000, 20 wt% in water) were purchased from Sigma-Aldrich Chemicals Co. (St. Louis, MO, USA). Cysteamine and poly(*N*-vinyl-2-pyrrolidone) (PVP) (K30, M_w = 30 000–40 000) were obtained from Aladdin Chemical Co. (Shanghai, China). Graphite powder, sodium citrate dihydrate ($C_6H_5Na_3O_7 \cdot 2H_2O$), sodium borohydride ($NaBH_4$), chloroauric acid ($AuCl_3 \cdot HCl \cdot 4H_2O$), $AgNO_3$, K_2HPO_4, KH_2PO_4, NaCl, KCl and NaOH were purchased from Shanghai Chemical Reagents Co., Ltd. (Shanghai, China). AgNPs and AuNPs were prepared *via* a reduction reaction according to the respective literature reports.[16,25,26] PDDA-functionalized graphene oxide (P-GO) was fabricated according to the literature based on the Hummers and Offeman method.[16] *E. coli* was obtained from State Key Laboratory of Agricultural Microbiology, Huazhong Agricultural University. Luria broth (LB) medium contains 1.0% of tryptone, 0.5% of sodium chloride and 0.5% of yeast extract was used to culture bacteria. All other common solvents and salts were of analytical grade and used as received. Phosphate buffered saline (PBS) were prepared by mixing PB solutions with 0.9% NaCl. Ultrapure water (Mill-Q, Millipore, 18.2 MΩ resistivity) was used throughout the experiments.

Apparatus

Cyclic voltammetry (CV) and electrochemical impedance spectroscopy (EIS) were performed using a CHI 660b electrochemical workstation (China, Chenhua). All experiments were carried out using a conventional three-electrode system. A modified or bare Au electrode of 2 mm diameter, a platinum wire and an Ag/AgCl (saturated KCl) electrode were used as the working electrode, counter electrode and reference electrode, respectively.

The absorption spectra were acquired on a TU-1901 UV-vis spectrometer (Purkinje General Instrument Co., Ltd., China). Transmission electron microscopy (TEM) images were taken using a Hitachi-7650 transmission electron microscope (Hitachi Ltd., Japan) at an acceleration voltage of 200 kV. Scanning electron microscopy (SEM) samples were imaged using a JSM-6700F Scanning Electron Microscope (JEOL Ltd., Japan). Zeta-potential measurements were measured using a Zetasizer Nano ZS90 DLS system (Malvern Instruments Ltd., UK).

Bacteria cultivation and plate count method

E. coli was cultured in LB medium at 37 °C for 24 h and serially diluted to 10^{-9} using normal saline solution. Conventional

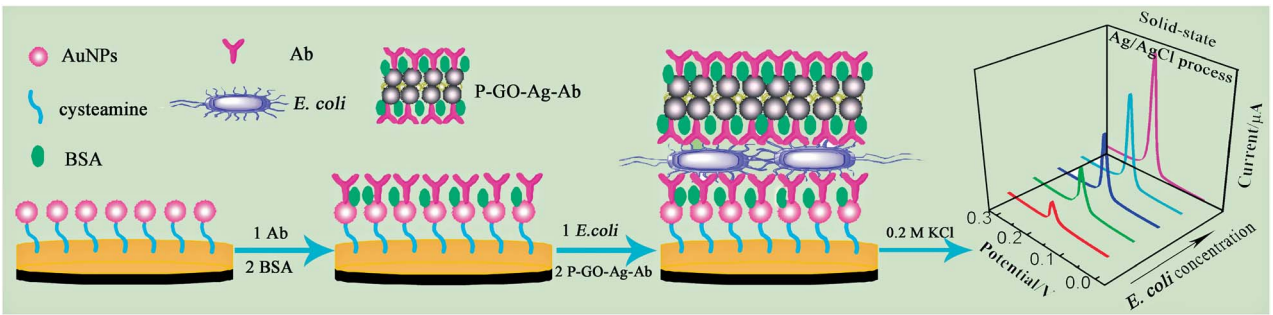

Fig. 1 Schematic image of the *E. coli* sensing strategy.

plate counting method was applied to determine the concentration of colony-forming units (cfu) in the bacteria solutions. One hundred microliters of the dilution were plated on LB agar and incubated at 37 °C for 48 h. Finally, *E. coli* colonies on the plate were counted to determine the number of colony-forming units per milliliter (cfu mL^{-1}).

Preparation of P-GO–Ag composites

The P-GO–Ag composites were synthesized based on a previous method.[16] Forty microliters of 1 mg mL^{-1} P-GO were added to 1.5 mL of as-prepared AgNPs under stirring. Then the solution was sonicated for 3 min before allowing to stand overnight. The precipitate was washed several times and redispersed in 1 mL of PBS (pH 7.4) for further use.

Immobilization of Ab onto P-GO–Ag composites

P-GO–Ag–Ab conjugates were prepared by the addition of 20 μL of anti-*E. coli* Ab (500 μg mL^{-1}) to 1.0 mL of P-GO–Ag colloid. After shaking for 60 min at room temperature, the uncoated sites were blocked with 100 μL of 2% BSA in PBS and incubated at 4 °C overnight. After centrifugation, the supernatant was removed and the precipitate was resuspended in 500 μL of PBS with 0.2% BSA for the following experiment.

Immunoreaction and measurement procedure

The whole immunoassay process was schematically illustrated in Fig. 1. Prior to use, the Au electrode was carefully disposed according to the procedure described in our previous work.[24] The pretreated electrode was immersed in 0.1 M cysteamine aqueous solution for 10 h, followed by washing with water, and then placed in the gold colloid at 4 °C. After 8 h, the AuNPs-modified electrode was rinsed with water. Subsequently, it was incubated with 10 μL of 50 μg mL^{-1} Ab at 4 °C for 12 h with 100% humidity and washed thoroughly with PBST (PBS with 0.05% Tween, pH 7.4) to remove the non-specifically bonded Ab. After blocking with 2 wt% BSA at 37 °C for 1 h and washing with PBST, the electrode was incubated with an *E. coli* sample at a certain concentration for 1 h at 37 °C. Afterwards, 10 μL of P-GO–Ag–Ab bioconjugates was pipetted onto the modified electrode and maintained for another 1 h at 37 °C. Before CV measurement, the fabricated biosensor was rinsed thoroughly with PBST to remove the physically adsorbed nanoprobe of P-GO–Ag–Ab.

Results and discussion

Characteristics of P-GO–Ag composites

The P-GO–Ag composites were confirmed by the UV-vis absorption spectrum as shown in Fig. 2A. The P-GO (curve a) displayed a strong absorption peak at 230 nm and a shoulder peak at 300 nm, which corresponded to π → π* transitions of the aromatic C=C bond and n → π* transition of the C=O bond, respectively.[27] After being decorated with AgNPs, P-GO–Ag composites showed a characteristic peak of AgNPs at 396 nm, which indicated the successful capture of the AgNPs. The typical TEM image presented in Fig. 2B also demonstrated

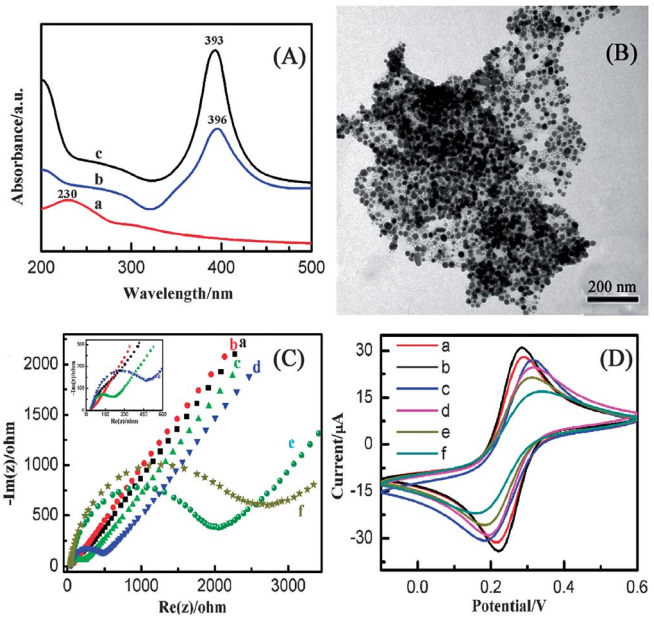

Fig. 2 (A) Absorption spectra of (a) P-GO, (b) P-GO–Ag and (c) Ag nanoparticles. (B) TEM images of P-GO–Ag composites. (C) EIS and (D) CV of the electrode at different stages in 0.5 M KCl + 5.0 mM $[Fe(CN)_6]^{3-}$: (a) bare Au electrode, (b) AuNPs/Au electrode, (c) Ab/AuNPs/Au electrode, (d) BSA/Ab/AuNPs/Au electrode, (e) *E. coli*/BSA/Ab/AuNPs/Au electrode and (f) Ab/*E. coli*/BSA/Ab/AuNPs/Au electrode.

the formation of the composites. It was observed that all P-GO nanosheets were decorated with AgNPs and nearly all the AgNPs were distributed uniformly on the both sides of nanosheets. This high-efficiency self-assembly was due to the strong electrostatic interaction between P-GO and the AgNPs, which was verified by the results of zeta-potential measurement. The mean zeta-potential of P-GO was positive (+44.3 mV) due to the modification of PDDA, whereas that of the AgNPs was negative (−37.5 mV) owing to the capping reagent of sodium citrate. So a large number of AgNPs could be adsorbed on both sides of the P-GO by the strong electrostatic interaction between them. Moreover, the large amount of AgNPs modified on P-GO and the good affinity of AgNPs for biomolecules were both beneficial to increase the loading amount of Ab.[17]

Electrochemical characteristics of the immunosensor

The stepwise construction process of the immunosensor was characterized by EIS (Fig. 2C) and CV (Fig. 2D) in 0.5 M of KCl solution containing 5.0 mM of $[Fe(CN)_6]^{3-}$. Significant differences were observed in the electron-transfer resistance (R_{et}) upon the stepwise modification of the electrode (Fig. 2C). The bare Au electrode exhibited an almost straight line (curve a), indicating a fast charge-transfer process at the electrode. When the AuNPs were assembled, the EIS was similar to that of the bare electrode (curve b), which implied the excellent electrical conductivity of the AuNPs. Subsequently, the immobilization of Ab generated an insulating protein layer and enhanced the resistance (curve c). Followed by blocking with BSA (curve d), the EIS showed a higher resistance. In particular, when *E. coli*

was immobilized on the electrode through immunoreaction with the anchored Ab, the R_{et} significantly increased to about 2000 Ω (curve e). That could be attributed to the immense barrier from the bacteria fixed on the electrode surface. Finally, the largest R_{et} (curve f) was observed after further incubation with Ab. Fig. 2D shows the CVs of $[Fe(CN)_6]^{3-}$ on the modified electrode at different stages. On the bare Au electrode, a well-defined redox peak pair was observed (curve a). After immobilization of the AuNPs, the current increased due to the increment of electron transfer from the AuNPs. Subsequently the current response decreased and the peak-to-peak separation was enlarged after different objects were self-assembled on the electrode (curves c–f) step by step. The results of CV experiments were in good agreement with those of EIS experiments, confirming the success of each assembly step again.

SEM characterization of the immunosensor

To witness the fabrication of the immunosensor, we tracked the morphology changes of the gold-coated mica sheet, which was used to replace the Au electrode. As shown in Fig. 3, when AuNPs were assembled, clear mono-dispersed and spherical deposits could be seen (Fig. 3A). After Ab anchoring and BSA blocking, the surface became smoother (Fig. 3B), which might be ascribed to Ab and BSA filling the interstitial places on the above interface. In Fig. 3C, rod-shaped bacteria were obviously observed, indicating that *E. coli* could be fixed on the surface through the immunoreaction with the Ab. After the P-GO–Ag–Ab probes were recognized by *E. coli*, a thinnish sheet loaded with a number of bright dots coated the bacteria. These results further demonstrated that the biosensor could be fabricated successfully in this way.

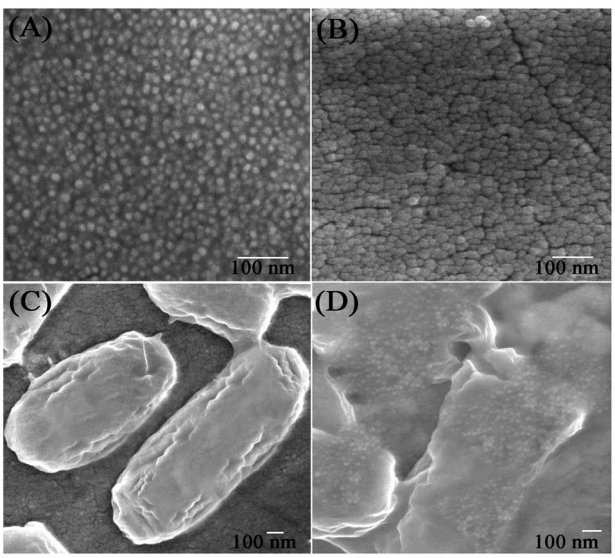

Fig. 3 SEM images of (A) AuNPs/gold-coated mica sheet, (B) BSA/Ab/AuNPs/gold-coated mica sheet, (C) *E. coli*/BSA/Ab/AuNPs/gold-coated mica sheet and (D) P-GO–Ag–Ab/*E. coli*/BSA/Ab/AuNPs/gold-coated mica sheet.

The advantage of solid-state voltammetry

Fig. 4A shows a stripping voltammogram in 1.0 M KNO_3 solution (curve a) and a solid-state voltammogram in 0.2 M KCl solution (curve b) from the similar amount of AgNPs (the detailed procedures were listed in the ESI†). It is observed that a much larger peak current was detected by solid-state voltammetry. Moreover, the electrooxidation of Ag in the solid-state Ag/AgCl process occurred at a much lower potential, where unwanted oxidative interferences were minimal and the contribution of the background current was very small. These results were possibly attributed to the following reasons. Firstly, when Cl^- was presented in the solution, Ag was oxidized to Ag^+ and formed the insoluble product of AgCl on the electrode surface instead of diffusing into solution. Also, the formation of insoluble AgCl ($K_{sp} = 1.77 \times 10^{-10}$ at 25 °C) induced the electrooxidation of Ag to occur at a quite low potential, which was approximately +0.14 V *vs.* Ag/AgCl electrode (saturated KCl). Secondly, since nucleation and growth were the rate-limiting steps in the Ag/AgCl solid-state voltammetric process, the process produced a sharper and more intense peak, as compared with other voltammetric processes.[21] Finally, the insoluble AgCl could not diffuse into solution and then be electroreduced to form Ag on the electrode surface. That resulted in the current response of Ag/AgCl solid-state voltammetry being very stable after scanning for 20 cycles. These unique advantages were beneficial for analytical applications.

Current response of the immunosensor using AuNPs and P-GO for amplification

A novel label based on P-GO and AgNPs was designed and detected by using the solid-state voltammetric technique to realize a sensitive, simple and rapid monitoring of bacterium, which had not yet been reported for the electrochemical assay of *E. coli*. The typical solid-state voltammetric response of the label in 0.2 M KCl is shown in Fig. 4B (curve a). As expected, two well-defined current peaks were observed, which corresponded to the oxidation of Ag and the reduction of AgCl, respectively.[20–24] Also, the great amplification of the current signal with AuNPs and P-GO–Ag labels is demonstrated in Fig. 4B. Compared with

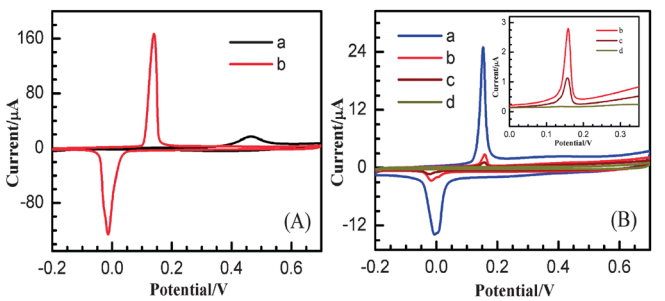

Fig. 4 (A) (a) Solid-state voltammogram of Ag/AgCl process in a 0.2 M KCl solution and (b) silver stripping voltammogram in 1.0 M KNO_3 solution. (B) Typical voltammetric response of the (a) P-GO–Ag–Ab/*E. coli*/BSA/Ab/AuNPs/Au electrode, (b) P-GO–Ag–Ab/*E. coli*/BSA/Ab/Au electrode, (c) Ag–Ab/*E. coli*/BSA/Ab/AuNPs/Au electrode and (d) P-GO–Ag–Ab/BSA/Ab/AuNPs/Au electrode; concentration of *E. coli*: 10^5 cfu mL^{-1}, scan rate: 0.1 V s^{-1}.

P-GO–Ag–Ab/*E. coli*/BSA/Ab/Au (the capture Ab was coated on Au electrode directly) and Ag–Ab/*E. coli*/BSA/Ab/AuNPs/Au (the AgNPs bonded directly with Ab and were used as the label), P-GO–Ag–Ab/*E. coli*/BSA/Ab/AuNPs/Au was highly enhanced 9.95-fold and 26.92-fold, respectively. That could be attributed to the high-loading capability of graphene oxide and promoting the electron-transfer rate of the AuNPs. Furthermore, in a control experiment, there is no distinct peak observed (Fig. 4B, curve d). These results further demonstrated that the promoted electron-transfer rate of the AuNPs and the increased AgNPs loading of the P-GO–Ag labels could dramatically improve the peak current whilst not enhancing the background.

Additionally, the effect of different concentration of KCl on the peak width at half height and peak height were investigated. The results in Fig. 5 showed that the peak width at half height became smaller at a higher concentration; also, the peak current was reduced when the concentration of KCl was larger than 0.2 M. Therefore, 0.2 M KCl was chosen for this study.

Sensitivity of the immunosensor

On the basis of the optimal conditions, the sandwiched immunoassay was applied for the detection of *E. coli*. Fig. 6 depicts the current response from the immunosensor after reacting with different concentrations of *E. coli*. As could be seen, the peak current increased with the increase of *E. coli* in the range of 20–1.0×10^8 cfu mL^{-1}, and the calibration curve is linear in a wide range from 50 to 1.0×10^6 cfu mL^{-1}. The regression equation was $Y = -11.37 + 7.04X$ with $R = 0.999$. The detection limit was 10 cfu mL^{-1} with a signal-to-noise ratio of 3. Furthermore, compared with some other electrochemical immunoassays for the determination of *E. coli*, the present immunosensor displayed a relatively wide linear detection range and low detection limit (shown in Table S1 in ESI†).

Specificity, reproducibility and stability of the immunosensor

The specificity test was conducted by using different microorganisms such as *Bacillus subtilis* (1.8×10^4 cfu mL^{-1}), *Enterobacter aerogenes* (2.0×10^4 cfu mL^{-1}) and *Enterobacter dissolvens* (2.5×10^4 cfu mL^{-1}) as controls. As shown in Fig. 7, the current signals for *B. subtilis*, *E. aerogenes* and *E. dissolvens* were 0.946, 1.124, and 1.503 μA, respectively, whereas it was 17.300 μA for *E. coli* (1.0×10^4 cfu mL^{-1}). The results

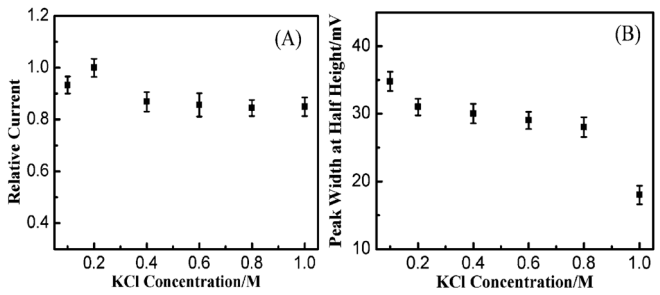

Fig. 5 Effect of concentration of KCl on (A) the peak current normalized by peak height obtained in 0.2 M KCl and (B) the peak width at half height.

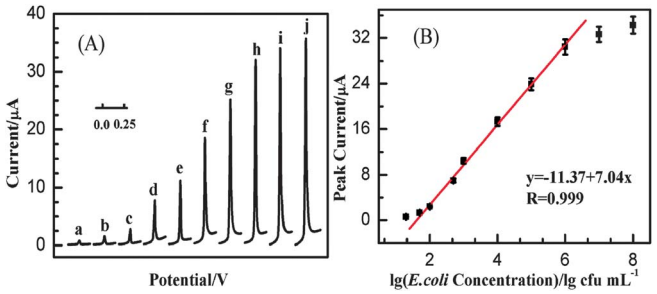

Fig. 6 (A) The current response of the immunosensor in different concentrations of *E. coli* (cfu mL^{-1}): (a) 20, (b) 50, (c) 1.0×10^2, (d) 5.0×10^2, (e) 1.0×10^3, (f) 1.0×10^4, (g) 1.0×10^5, (h) 1.0×10^6, (i) 1.0×10^7 and (j) 1.0×10^8. (B) A linear calibration plot between the current response and the logarithmic value of *E. coli* concentration.

demonstrated that the response induced by the non-specific bonding was much lower than the response caused by the specific immunoreaction. Hence, the immunosensor for *E. coli* was specific, and the presence of other related microorganisms did not provide significant interference. The reproducibility of the biosensor was also investigated with three biosensors prepared independently under the same experimental conditions. The variation coefficients obtained were 8.47%, which indicated that the immunosensor possessed acceptable reproducibility. Furthermore, we found that the immunosensor retained 90.5% of original current response after 10 days of storage in 0.01 M PBS at 4 °C, indicating the good stability of the immunosensor.

Detection of *E. coli* in lake water

To further investigate the feasibility of the immunosensor for applications in environment monitoring, the sensing of *E. coli* in lake water was carried out. Before the determination, a liter of the samples was filtered using a 0.45 μm pore size filter to enrich *E. coli*. Then the filter was placed in a flask containing 4 mL PBS buffer (pH 7.4), and the gathered *E. coli* was detected using the proposed immunoassay. The results of five independent samples were given in Table 1. It was clearly observed that the concentrations of *E. coli* were tested as 324, 240, 304, 280 and 248 cfu L^{-1} in the water sample before enrichment, respectively, which were close to the results obtained by the plate counting method.

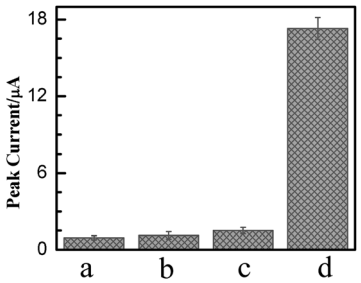

Fig. 7 The current response for (a) *B. subtilis* (1.8×10^4 cfu mL^{-1}), (b) *E. aerogenes* (2.0×10^4 cfu mL^{-1}), (c) *E. dissolvens* (2.5×10^4 cfu mL^{-1}) and (d) *E. coli* (1.0×10^4 cfu mL^{-1}).

Table 1 Comparison of the proposed detection results of real water samples between the immunoassay and plate counting methods

Water sample	Plate counting methods/cfu L^{-1}	This method/cfu L^{-1}
1	304	324
2	220	240
3	280	304
4	288	280
5	232	248

Conclusion

With the signal amplification of the promoted electron-transfer rate of the AuNPs and the increased AgNPs loading of the P-GO–Ag–Ab probes, a new electrochemical immunoassay for *E. coli* has been proposed. In this protocol, a solid-state voltammetric technique has been first introduced for the detection of bacteria. Integrating the advantages of sensitive solid-state voltammetric detection, specific immunoreaction with a nanoparticle amplification technique, the constructed immunosensor showed a good analytical performance for *E. coli*. Real samples have been performed and the results obtained are in good agreement with the plate counting methods. Based on these results, it is demonstrated that the developed immunoassay could be used for the detection of *E. coli* in water samples. We anticipated that our sensing strategy would be extended for the determination of other bacteria and opens a new avenue for the design of electrochemical sensors.

Acknowledgements

We gratefully acknowledge the financial support from National Natural Science Foundation of China (21175051), the Fundamental Research Funds for the Central Universities (2011PY139) and the Natural Science Foundation of Hubei Province Innovation Team (2011CDA115).

References

1 J. Y. Lim, J. Yoon and C. J. Hovde, *J. Microbiol. Biotechnol.*, 2010, **20**, 5.
2 C. L. Moe, M. D. Sobsey, G. P. Samsa and V. Mesolo, *Bull. W. H. O.*, 1991, **69**, 305.
3 M. A. Hood and G. E. Ness, *Appl. Environ. Microbiol.*, 1982, **43**, 578.
4 K. F. Eckner, *Appl. Environ. Microbiol.*, 1998, **64**, 3079.
5 A. P. Dufour, E. R. Stricklanda and V. J. Cabelli, *Appl. Environ. Microbiol.*, 1981, **41**, 1152.
6 R. C. Li, D. E. Nix and J. J. Schentag, *Antimicrob. Agents Chemother.*, 1993, **37**, 371.
7 Z. Q. Shen, J. F. Wang, Z. G. Qiu, M. Jin, X. W. Wang, Z. L. Chen, J. W. Li and F. H. Cao, *Biosens. Bioelectron.*, 2011, **26**, 3376.
8 C. Y. Si, Z. Z. Ye, Y. X. Wang, L. Gai, J. P. Wang and Y. B. Ying, *Spectrosc. Spectral Anal.*, 2011, **31**, 2598.
9 S. A. Kalele, A. A. Kundu, S. W. Gosavi, D. N. Deobagkar, D. D. Deobagkar and S. K. Kulkarni, *Small*, 2006, **2**, 335; B. Guven, N. Basaran-Akgul, E. Temur, U. Tamer and İ. H. Boyacı, *Analyst*, 2011, **136**, 740; E. Temur, İ. H. Boyacı, U. Tamer, H. Unsal and N. Aydogan, *Anal. Bioanal. Chem.*, 2010, **397**, 1595.
10 P. Geng, X. A. Zhang, W. W. Meng, Q. J. Wang, W. Zhang, L. T. Jin, Z. Feng and Z. R. Wu, *Electrochim. Acta*, 2008, **53**, 4663; P. Geng, X. A. Zhang, Y. Q. Teng, Y. Fu, L. L. Xu, M. Xu, L. T. Jin and W. Zhang, *Biosens. Bioelectron.*, 2011, **26**, 3325; Q. Y. Yang, Y. Liang, T. S. Zhou, G. Y. Shi and L. T. Jin, *Electrochem. Commun.*, 2009, **11**, 893; L. J. Yang, Y. B. Li and G. F. Erf, *Anal. Chem.*, 2004, **76**, 1107.
11 Y. Q. Teng, X. A. Zhang, Y. Fu, H. J. Liu, Z. C. Wang, L. T. Jin and W. Zhang, *Biosens. Bioelectron.*, 2011, **26**, 4661.
12 X. A. Zhang, P. Geng, H. J. Liu, Y. Q. Teng, Y. J. Liu, Q. J. Wang, W. Zhang, L. T. Jin and L. Jiang, *Biosens. Bioelectron.*, 2009, **24**, 2155.
13 J. Wang, *Analyst*, 2005, **130**, 421.
14 G. D. Liu and Y. H. Lin, *Talanta*, 2007, **74**, 308; J. Wang, H. Y. Han, X. C. Jiang, L. Huang, L. N. Chen and N. Li, *Anal. Chem.*, 2012, **84**, 4893.
15 Y. H. Lin, S. H. Chen, Y. C. Chuang, Y. C. Lu, T. Y. Shen, C. A. Chang and C. S. Lin, *Biosens. Bioelectron.*, 2008, **23**, 1832.
16 W. Ren, Y. X. Fang and E. K. Wang, *ACS Nano*, 2011, **5**, 6425.
17 K. P. Liu, J. J. Zhang, C. M. Wang and J. J. Zhu, *Biosens. Bioelectron.*, 2011, **26**, 3627.
18 D. Du, L. M. Wang, Y. Y. Shao, J. Wang, M. H. Engelhard and Y. H. Lin, *Anal. Chem.*, 2011, **83**, 746.
19 X. Y. Yang, X. Y. Zhang, Z. F. Liu, Y. F. Ma, Y. Huang and Y. S. Chen, *J. Phys. Chem. C*, 2008, **112**, 17554.
20 B. P. Ting, J. Zhang, Z. Q. Gao and J. Y. Ying, *Biosens. Bioelectron.*, 2009, **25**, 282.
21 B. P. Ting, J. Zhang, M. Khan, Y. Y. Yang and J. Y. Ying, *Chem. Commun.*, 2009, 6231.
22 J. Zhang, B. P. Ting, N. R. Jana, Z. Q. Gao and J. Y. Ying, *Small*, 2009, **5**, 1414.
23 G. S. Lai, J. Wu and H. X. Ju, *Adv. Funct. Mater.*, 2011, **21**, 2938.
24 X. C. Jiang, K. Chen and H. Y. Han, *Biosens. Bioelectron.*, 2011, **28**, 464.
25 P. C. Lee and D. Meisel, *J. Phys. Chem.*, 1982, **86**, 3391.
26 G. Frens, *Nature*, 1973, **241**, 20.
27 J. L. Chen and X. P. Yan, *J. Mater. Chem.*, 2010, **20**, 4328.